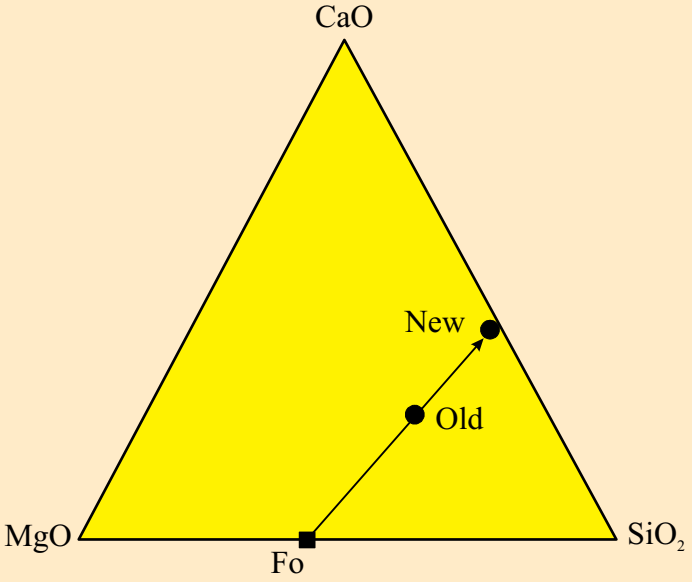

Figure 1. Triangular diagram illustrating the process of crystal fractionation in a simple system. Old is the composition of the original melt. New is the composition of a new melt that forms as the result of frationating forsterite from the old melt until the ratio of solid to liquid is 2/3.

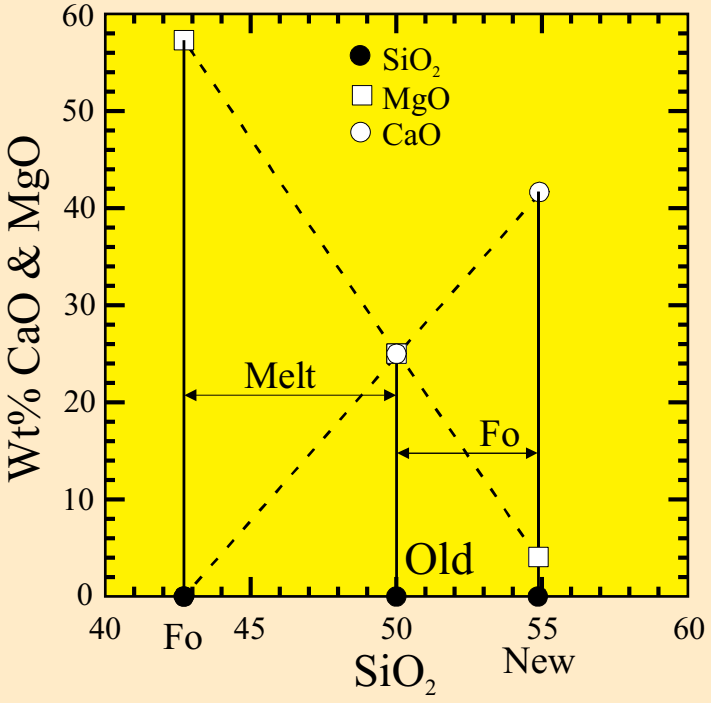

Figure 2. Addition-Subtraction diagram for the data in Table 1. An addition-subtraction diagram is an alternate way of describing crystal fractionation that can be extended to more complex compositions.

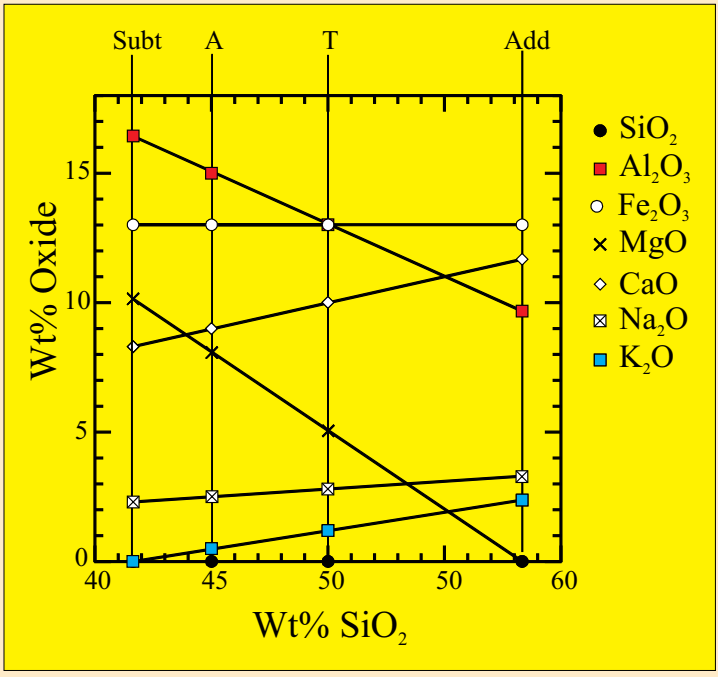

Figure 3. Addition-subtraction diagram that illustrates the initial use of such a diagram by Bowen (1928). See text and Bowen's book for explanation.

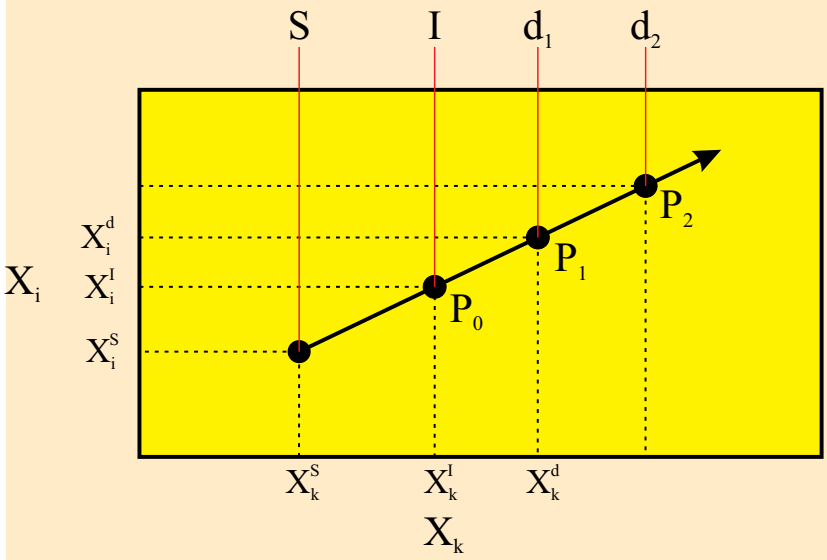

Figure 4. Diagram that shows the mathematical notation for the variables in the equations for addition-subtraction diagrams.

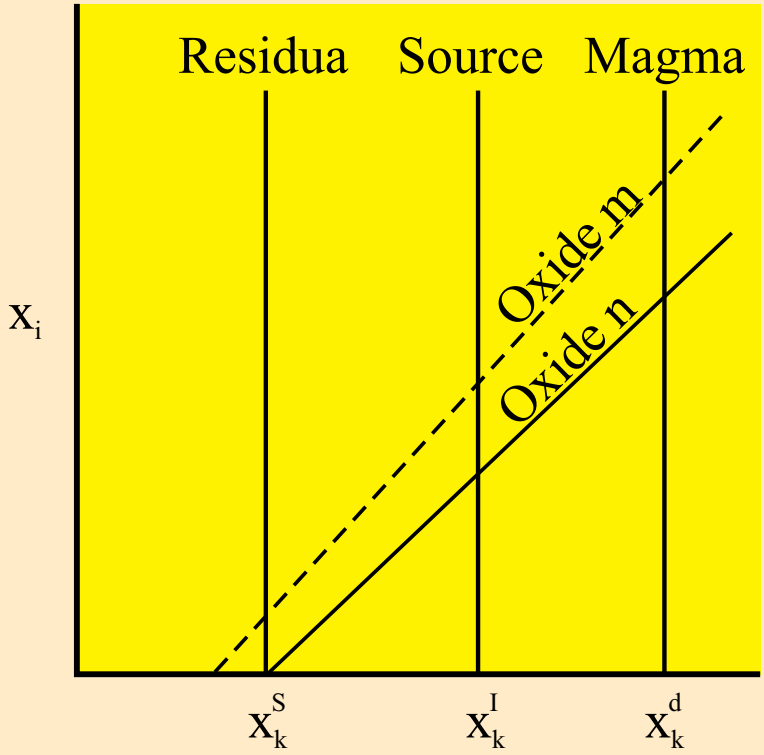

Figure 5. Diagram that shows how to select the value for the independent variable in the residue from the partial melting of a source composition that produces the composition of the magma. This is the maximum amount of partial melting possible, given the source and magma compositions. The dashed line starts at a value of the independent variable that would cause the residue to have negative values for some constituents.

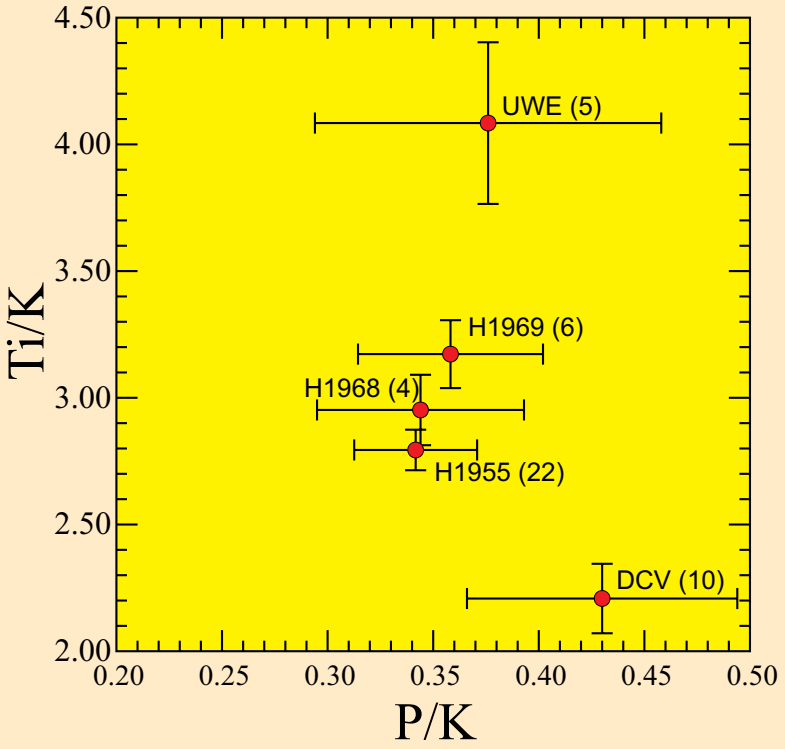

Figure 6. Plot of Ti/K vs P/K for some Kilauea rocks: [Prehistoric Uwekahuna Laccolith (UWE); Historic lava flows from eruptions in 1955, 1968, and 1969] and Diamond Craters volcanic field in Oregon. The error bars are ± one standard deviation within each data set. Numbers in parentheses indicate the numbers of samples in each set.

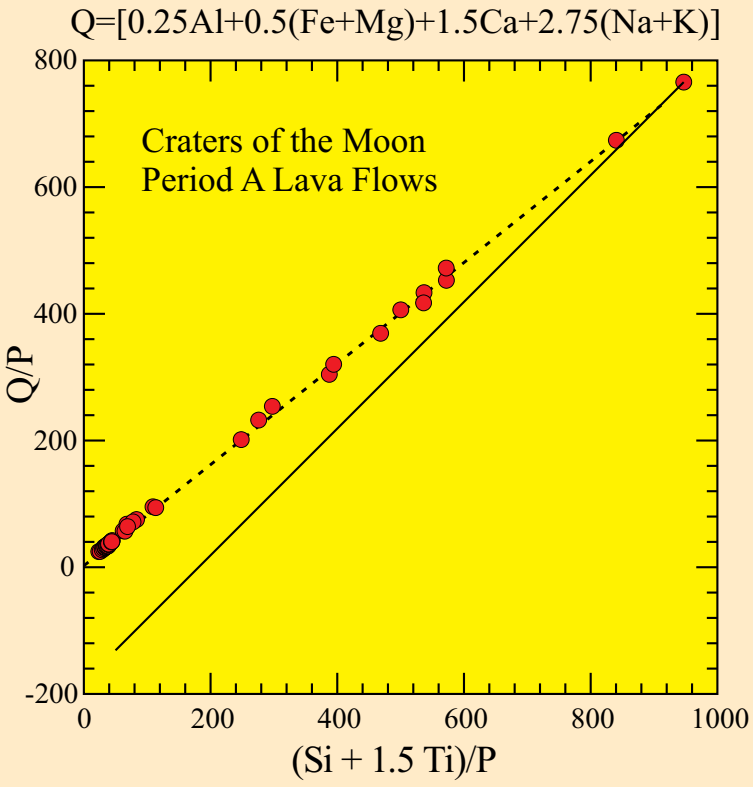

Figure 7. Element ratio diagram with a denominator that is not conserved in the data that plots closer to the origin. The different trends are defined by a discontinuity. The data closer to the origin define a trend through the origin (dashed line).

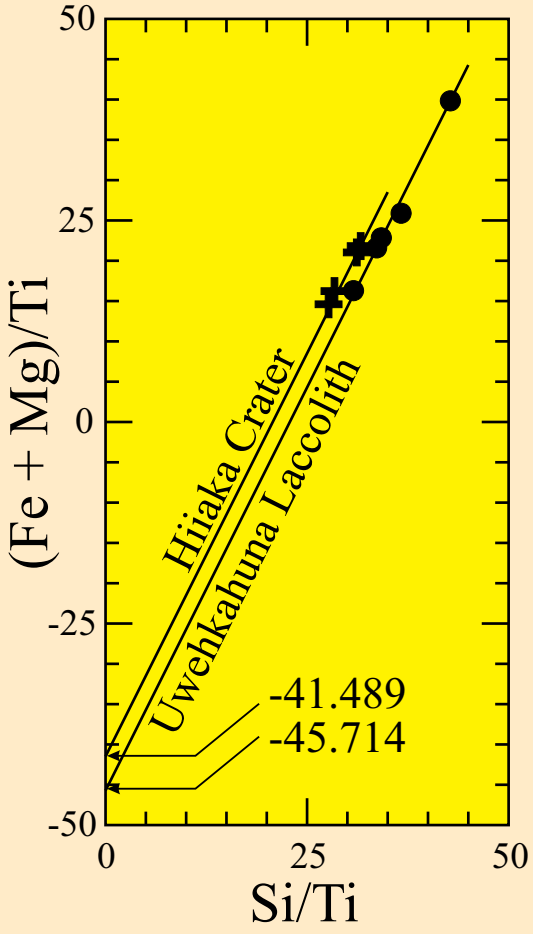

Figure 8. Plot of 0.5(Fe + Mg)/Ti vs Si/Ti for two picritic magma batches. The data from the two magma batches have different intercepts. Data from Murata and Richter (1971) and Wright(1971).

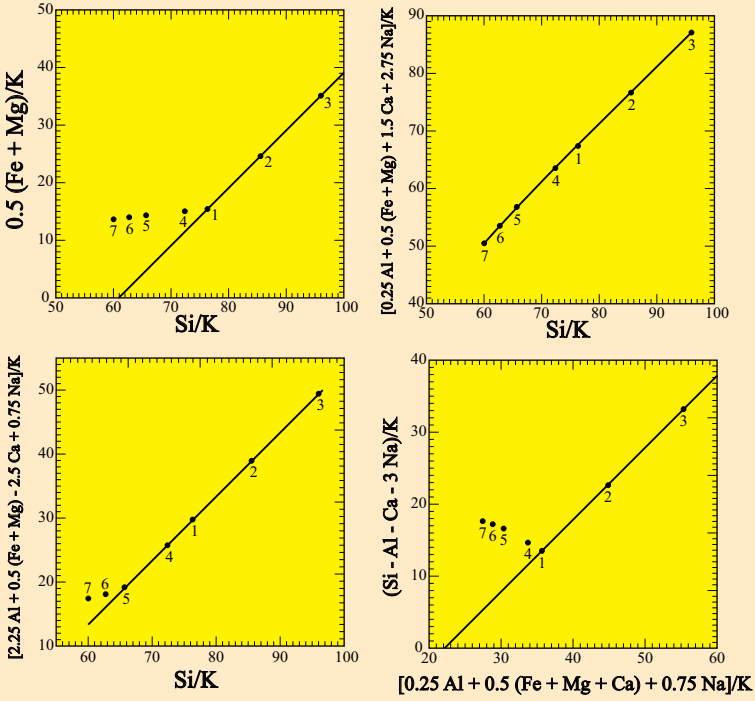

Figure 9. Pearce element ratio diagrams constructed from the data in Table 3. The lines all have a slope of one. See text for discussion and interpretation.

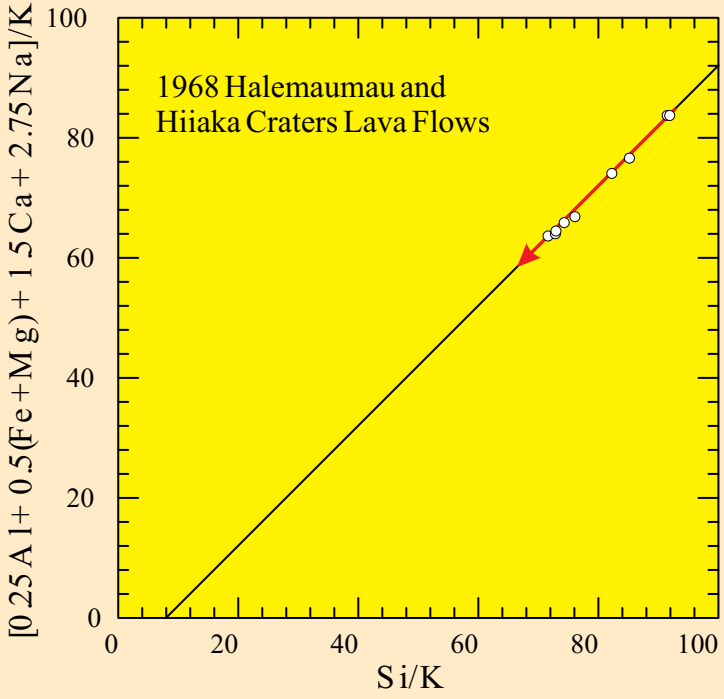

Figure 10. A Pearce element diagram to test whether the chemical variations can be the result of sorting (fractionation or accumulation) of olivine, plagioclase, and clinopyroxene. The arrow indicates the trend the data should follow if fractionation of olivine, plagioclase, and clinopyroxene caused the chemical variations in the rocks (Data fromWright, 1971; Wright and Fiske, 1971; Wright, et al., 1975. See also Nicholls and Stout, 1988).

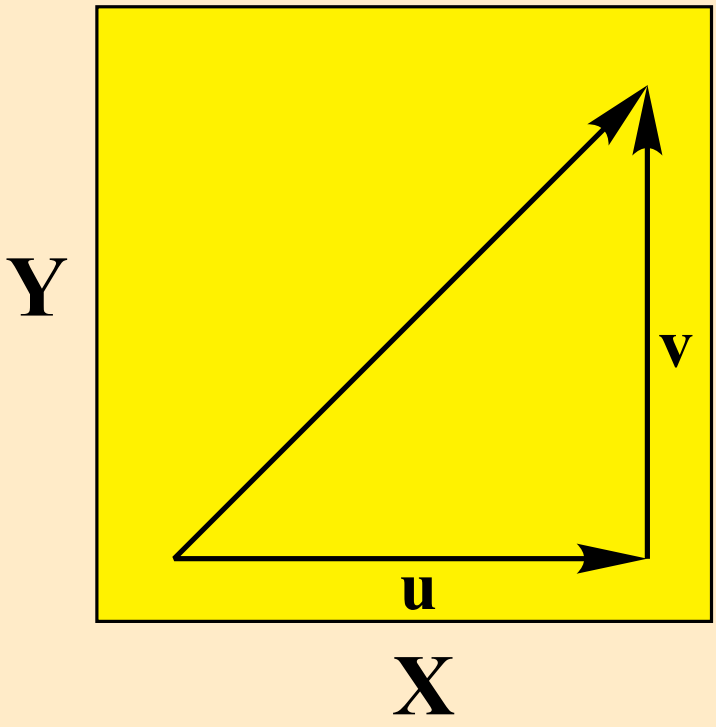

Figure 11. Schematic diagram showing the notation and relationships of the variables in Eqn. (24).

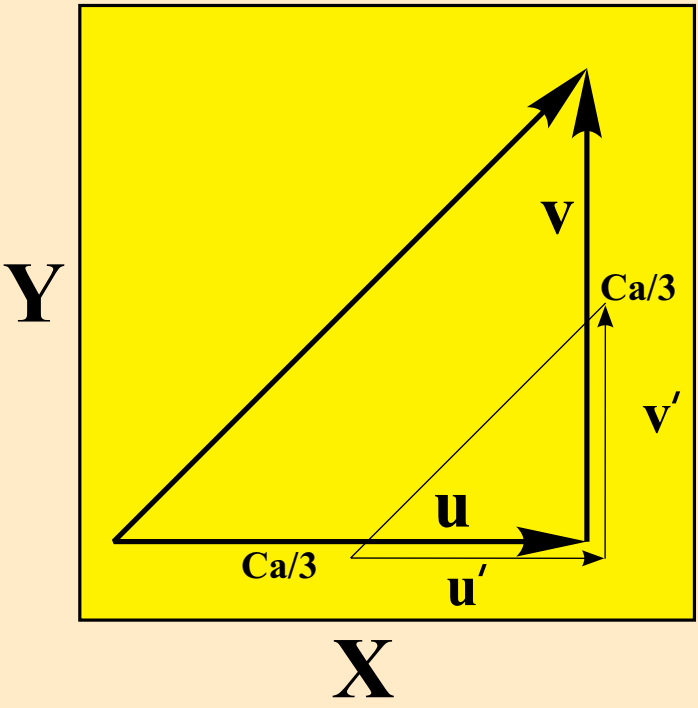

Figure 12. Schematic diagram showing the effect of moving an element, Ca, from the numerator on the X-axis to the numerator on th Y-axis.

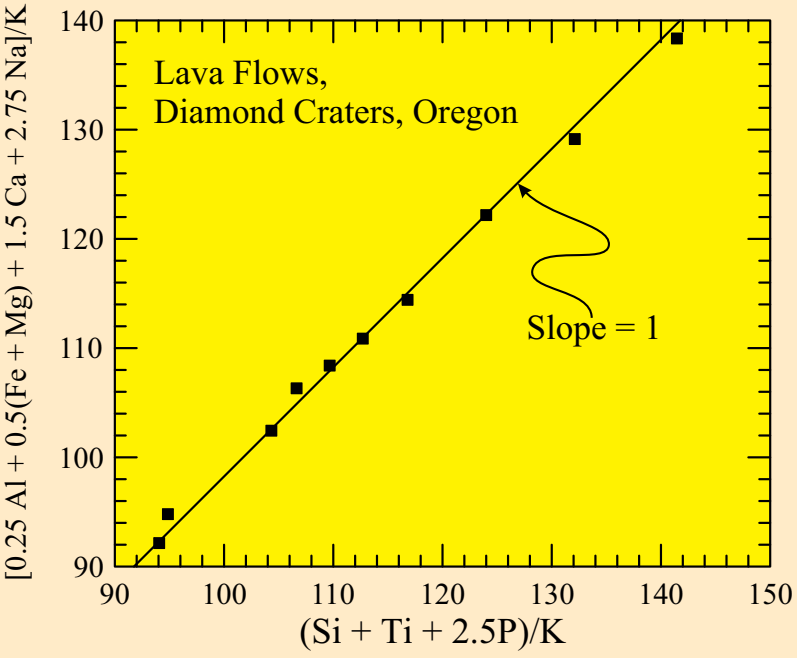

Figure 13. Pearce element ratio diagram derived for a phase composition matrix with N phases (end members) and N elements. The rank of the composition matrix is less than N because of the linear dependence of some of the phases (end members). Data from Russell and Nicholls (1987).

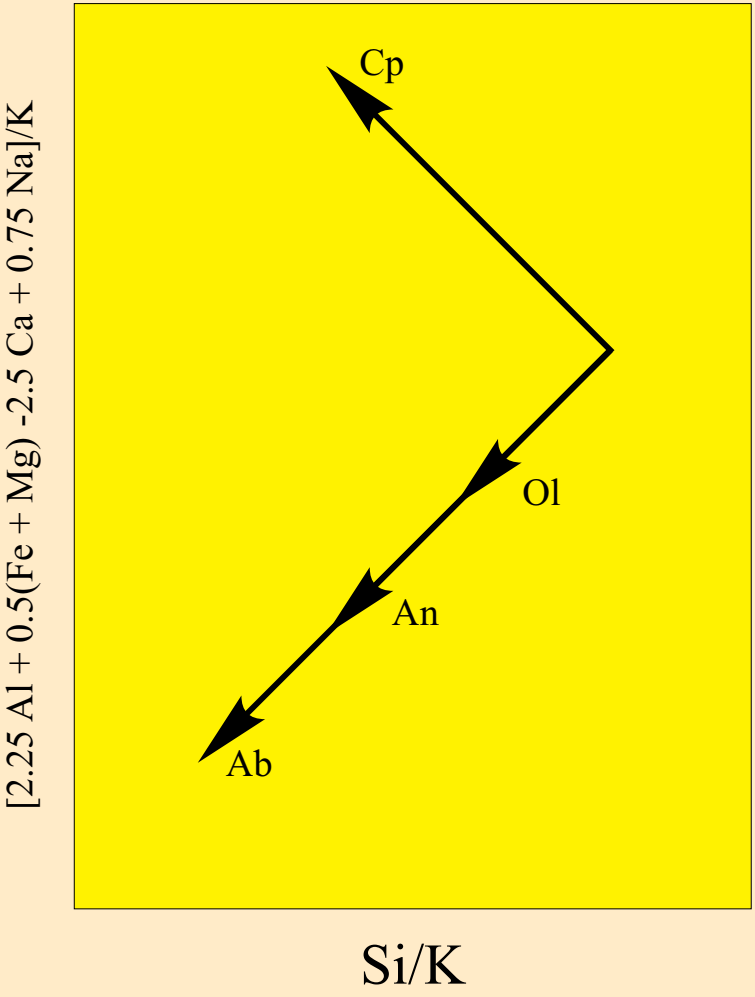

Figure 14. Schematic diagramshowing displacement vectors for testing whether clinopyroxene is part of a sorting assemblage that also includes plagioclase and olivine. Ab = albite, An = anorthite, Cp = clinopyroxene, Ol = olivine.

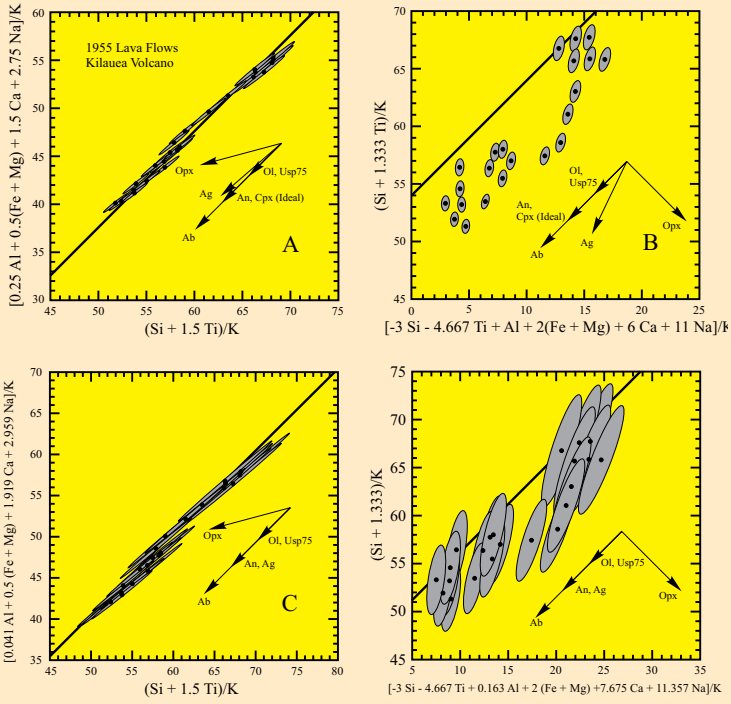

Figure 15. Pearce element ratio diagram testing whether orthopyroxene (Opx) is part of the sorted assemblage. Data from Macdonald and Eaton (1964); Wright and Fiske (1971). Ab = albite; An = anorthite; Cp(Ideal) = Ca(Mg,Fe)Si2O6; Ol=olivine; Usp=ulvospinel; Ag=augite with composition listed in Table 5.